OATAO

Open Archive Toulouse Archive Ouverte

OATAO is an open access repository that collects the work of Toulouse researchers and makes it freely available over the web where possible

This is an author's version published in: http://oatao.univ-toulouse.fr/25385

Official URL:

To cite this version:

A flood mitigation control strategy based on the estimation of hydrographs and volume dispatching [★]

B. Hadid [*] **E. Duviella** [*] **P. Chiron** [**] **B. Archimède** [**]

[*] *IMT Lille Douai, University of Lille, F-59000 Lille, France (e-mail: {baya.hadid,eric.duviella}@imt-lille-douai.fr)*
[**] *ENIT-LGP, Tarbes, France (e-mail: {pascale.chiron,bernard.archimede}@enit.fr)*

Abstract: Flood events are expected more frequent with biggest magnitude in the near future. They have potential big impacts on human economic activity and property, on health and life of man, and on the environment. One possibility to mitigate the flood impact consists in using flood storage areas and in designing a control strategy to dispatch the volumes of water and reducing the flow peak. The designed mitigation control strategy is based on the prediction of hydrographs and the estimation of the water volumes that have to be stored. It leads to optimal flow peak reduction according to the capacity of the flood storage areas. This paper details the steps of the proposed approach. Then, a realistic case-study is considered to illustrate the designed flood mitigation control strategy.

Keywords: Water systems, Flood, Control strategy, Flood storage areas, Large-scale systems.

1. INTRODUCTION

Based on recent tragic events in Europe, it is recognized that flood has a big impact on human economic activity and property, on health and life of man, and on the environment. Unfortunately, the frequency and the magnitude of flood are expected higher in near future according to several studies (Sauquet and Lang, 2017; Mustafa et al., 2018). The recommendation of the IPCC is to reduce the human's activities and the greenhouse gases in order to restrict global warming to 1.5 degrees and consequently limit the extreme weather events (IPCC, 2018). Pending required global political decisions to achieve this objective, flood mitigation solutions have be designed and proposed in the literature, in order to reduce water volumes and the flood peak. Some methods include optimization and multi-objective algorithms with different concepts such as scheduling, stochastic dynamic programming, evolutionary algorithms, meta-heuristics (Labadie, 2004; Zhang et al., 2019). Other authors adopt control strategies such as model predictive control method (MPC) using rainfall forecasts and predictions of river flow conditions ; combining MPC with Kalman filter (Breckpot et al., 2013; Delgoda et al., 2013) or with a reduced genetic algorithm in order to take into account the conceptual model uncertainties (Vermuyten et al., 2018). The coupling of optimization, regulation methods, as well as hydraulic simulation models, allow the generation of efficient strategies (Che and Mays, 2017; Raso et al., 2019; Shenava and Shourian, 2018). Flood decrease control strategies based on graph theory and optimization techniques are proposed in (Bencheikh et al., 2017; Nouasse et al., 2013). They lead to limit the flow peak by supplying and emptying flood storage areas. The purpose of this paper is to propose a flood mitigation control strategy combining a rainfall/runoff forecasting model, a water volume

estimation from the flood hydrograph and logic control rules, designed for generating the control setpoints of the reservoir gates in order to limit the effects of a flood.

The paper is organized as follows: the objectives of the method are given in Section 2. The flood limitation control strategy is detailed in Section 3. The proposed methodology is tested on a realistic case-study in Section 4 and simulation are presented. Finally, Section 5 draws conclusions and outlines future steps.

2. OBJECTIVES OF THE FLOOD MITIGATION

Strong rain events increase the discharge of rivers and canals and therefore their level. If the discharge is too high, according to the height of the river banks, flood can occur caused by overflows. With a good prediction of these events, it is possible to use adaptive water resource management strategies (Duviella et al., 2018). They consist in dispatching the water volume among the network by controlling hydraulic devices with the aim to keep the levels below the edges of the banks. In some case, the discharges are too high to allow the dispatching of the water volumes among the network avoiding floods. Flood storage areas offer thus a mitigation solution. These areas can be used as temporal tanks that are supplied during high flow periods and released after the occurrence of the extreme weather events. Even if using flood storage areas does not prevent totally floods, they limit their impacts thanks to the reduction of the flood peaks. Hence, flood mitigation control strategies have to be designed to optimize the use of storage areas.

The flood mitigation control strategy is part of the architecture depicted in Fig. 1. It requires rainfall data and hydrological models to determine the effect of rain on the discharge of the rivers and canals. Also, it requires predictive rainfall/runoff models to use predictive and adaptive control strategies. The
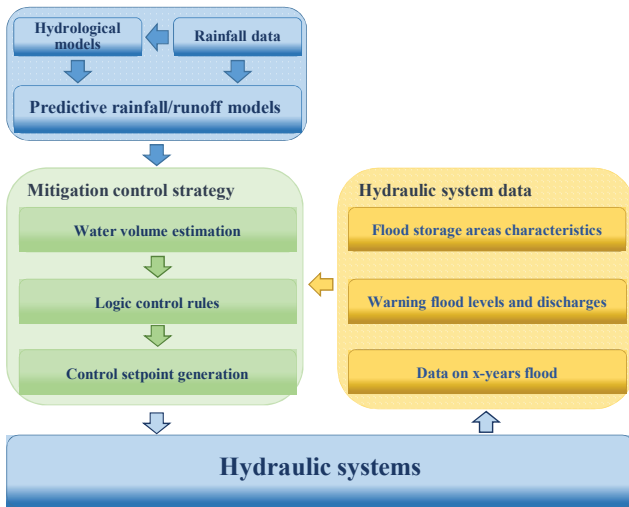
Fig. 1. Architecture of the flood mitigation control strategy .

flood mitigation control strategy depends also on the characteristics of the hydraulic systems that are composed of the rivers and the flood storage area. The value of the water volume that can be stored in the flood storage area is required. The warning flood levels and discharges must to be known. The flood storage areas can be designed according to different return periods if enough space is available. This information is required to design flood mitigation control strategy.

Based on the predictive rainfall/runoff models, an algorithm allows the estimation of the corresponding water volume. It aims at anticipating the use of the flood storage areas. The mitigation control strategy depends on some logic control rules that are specified according to the characteristics of the storage areas, the hydraulic systems, the warning flood levels, the size and the type of the hydrograph. Thus, according to these data and algorithm, a module aims at generating the control setpoint of the gates that supply and empty the flood storage areas.

3. FLOOD MITIGATION CONTROL STRATEGY

3.1 Rainfall/runoff forecasting

Nonlinearities are the biggest challenge faced when one seeks for a complex large-scale natural system model that has to be reproducible, especially when we have a limited knowledge of the intrinsic phenomena and when this system is rarely the same, for example in terms of geophysical properties. This is particularly true when, only based on the knowledge of the precipitation measurement and forecast, the runoff of the river has to be modelled. Indeed, the formation process of a flood starting from precipitations in a natural catchment is one of the biggest challenges faces by hydrologists. (Perrin and Andréassian, 2001) assessed at least 19 existing daily rainfall-runoff models. The reason is that the water level or flow rate depends on the temperature, the evapotranspiration and the vegetative cover. Other factors affecting the runoff include soil permeability, the river slope, etc.

The common goal of all the rainfall-runoff modeling approaches is to provide a flood forecast with a minimum lead-time (time between its announcement and arrival). The main proposed approaches are either physical/mathematical with a huge number of parameters or based on data. Commercial soft-

ware packages such as MIKE [1] , SIC [2] and InfoWorks [3] solve numerically the equations of Saint-Venant but at the expense of a long simulation time. Recent studies show the added value of nonlinear modeling approaches. In the literature, rainfall-runoff models are based on machine learning approaches such as neural networks (Feng and Lu, 2010) and adaptive neuro fuzzy inference systems (Chang and Chang, 2006). A survey on data driven modeling techniques is presented in (Elshorbagy et al., 2010). Neural networks (ANNs), genetic programming, evolutionary polynomial regression, Support vector machines (SVM), M5 model trees, K-nearest neighbors, and multiple linear regression techniques are implemented and evaluated using daily stream flow data. The SVM approach was also explored in (Asefa et al., 2006), where a short-term stream flow prediction was performed on hourly data. Machine learning techniques shown respectable results but still require a huge database to achieve a correct training. More recently, a semi-automatic software tool was proposed by (Wolfs et al., 2015). It combines different model structures both physical (weir equations) and data-driven (ANNs, PieceWise Linear, etc.) depending on the river dynamics. Conceptual systems based on tanks are proposed in (Perrin et al., 2003) requiring the knowledge of the evapotranspiration and soil saturation information.

On the other hand, the most efficient parametric approaches are nonlinear and consist first in the Hammerstein model (Bastin et al., 2009; Romanowicz et al., 2008) but has a frozen structure that can not be adaptive to a change in the operational conditions and thus has to be frequently re-calibrated. Second, in the same family of parametric nonlinear models, the Linear Parameter Varying (LPV) approach was also explored (Previdi and Lovera, 2009; Hadid et al., 2018). These studies were motivated by (Young, 2003) who proposed a data-based mechanistic modeling of the rainfall-flow dynamics based on a State Dependent Parameter approach and show a dependency of the model parameters according to the past rainfall and flow measurements. However, to the best of the author's knowledge, none of these methods was applied and validated on a large database with hourly measurements that contain multiple extreme rainy events and floods. A recursive online estimation of a linear ARX and nonlinear ARX models was proposed in (Duviella and Bako, 2012) to estimate the hydrograph peaks of the river with a prediction horizon of 24 hours. The idea was to include the prediction horizon in the regression vector composed of past flow measurements and forecasted rain. This approach has been improved in (Hadid et al., 2018) by using a recursive instrumental variable and a LPV off-line estimation. The LPV modeling approach with a delayed level as scheduling variable leads to a good flood forecasting. It is used in this paper to forecast the hydrographs and then estimate the magnitude of the flood peaks and their occurrence time.

3.2 Logic control rules

The logic control rules aim at determining the best flood mitigation control strategy based on water volume due to the flood and the capacity of the storage areas. Usually a threshold, denoted Q_{lam}, is selected as the limit from which the flood storage areas can begin to be supplied. Initially, this threshold is tuned according to a selected return period of x-year flood. When the capacity of the storage areas, denoted V_r, is higher than the water volume due to the flood over Q_{lam}, denoted V_f, the

---

[1] https://www.mikepoweredbydhi.com
[2] http://sic.g-eau.net/?lang=en
[3] https://www.geomod.fr/en/water-modelling/infoworks-icm/

flood storage areas can be supplied as soon as the discharge of the hydraulic system Q_i is superior to Q_{lam}. Else, other control rules have to be defined with the objective to limit the flood peak. In this case, a new value of Q_{lam}, denoted Q'_{lam}, has to be determined.

3.3 Water volume estimation and control setpoint determination

Algorithm 1 is applied for the determination of the optimal Q'_{lam} for a double peak hydrograph instead of a unit hydrograph which will allow to extend the principle on a multiple peak hydrograph. A double flood is defined as two successive peaks with a transition flow between these two peaks, noted herein Q_{min}, greater than the nominal river water flow. Fig. 2 depicts the different significant values used in the Algorithm 1 in order to identify Q'_{lam} through the estimation of water volumes generated by a double flood. t_1, t_{sep} and t_2 are the times that correspond to the intersection points between the horizontal line defined by Q_{min} and the hydrograph. t_{sep} is then the separation time of the double flood into two simple floods. Hence, V_1 and V_2 are the volumes calculated by integrating the hydrograph between t_1 and t_{sep} for V_1 and between t_{sep} and t_2 for V_2. For a precise volume calculation, a Matlab routine called *trapz* based on a trapezoidal numerical integration which allows to integrate numeric data rather than functional expressions is used. Q_{p_1} and Q_{p_2} are respectively the values of the peaks *i.e.* the maximum values of each simple hydrograph Q_{f_1} and Q_{f_2} separately. For $Q_{p_2} > Q_{p_1}$ (respectively $Q_{p_1} > Q_{p_2}$) the water volume V'_2 (resp. V'_1) is calculated by means of a numerical integration of the hydrograph between t'_1 and t'_2 resulting from the intersection of the horizontal line defined by Q_{p_1} (resp. Q_{p_2}) and the hydrograph.
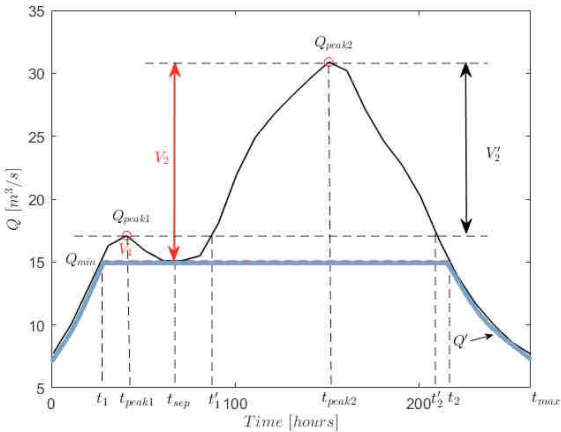

Fig. 2. Example of a double flood and its significant values used in the Algorithm 1.

If we take for example the case depicted in Figure 2 where $Q_{p_2} > Q_{p_1}$, Q'_{lam} can be located in three regions delimited by Q_{p_1} and Q_{min}: $Q_{p_1} \leqslant Q'_{lam} < Q_{p_2}$; $Q_{min} \leqslant Q'_{lam} < Q_{p_1}$; $Q'_{lam} \leqslant Q_{min}$. Since the calculation of Q'_{lam} is based on the knowledge of the reservoir volume V_r, an approximation of each unit hydrographs Q_{f_1} and Q_{f_2} by a predefined function is needed to calculate the integral and deduce Q'_{lam} value. More specifically, the upper side of each simple flood is first rotated counterclockwise by $\theta = 90°$ around a center located in the plane chosen arbitrarily as (t_{p_2}, Q_{p_2}) and translated along the y-axis to center in the horizontal direction and ensure a partial symmetry with respect to the x-axis. This operation allows to calculate the integral of the estimated function starting from the

flood peak value. The rotation is performed using Eq. (1), where $T_{1,2}$ is a time vector which values are the sampled time between t_1 and t_{sep} for Q_{f_1}, and t_{sep} and t_2 for Q_{f_2}, $Tr_{1,2}$; $Qr_{f1,2}$ are the rotation results of $T_{1,2}$ and $Q_{f1,2}$; I_d is an identity matrix of *ad hoc* dimension.

$$\begin{bmatrix} Tr_{1,2}^\top \\ Qr_{f1,2}^\top \end{bmatrix} = \begin{bmatrix} \cos(\theta) & -\sin(\theta) \\ \sin(\theta) & \cos(\theta) \end{bmatrix} \begin{bmatrix} T_{1,2}^\top - t_{p_2}.I_d \\ Q_{f1,2}^\top - Q_{p_2}.I_d \end{bmatrix} + \begin{bmatrix} t_{p_2} \\ Q_{p_2} \end{bmatrix} \quad (1)$$

Each part of the transformed hydrograph on both sides of x-axis is approximated by a polynomial function estimated using least squares algorithm. The polynomial degree chosen for each part is the one which gives the minimal estimation error norm. Let us consider P_{f1}^{up}, P_{f1}^{dw}, P_{f2}^{up} and P_{f1}^{dw} the polynomial functions that fit respectively the upper part of Q_{f_1} between t_{p_1} and t_{sep}, the symmetric with respect to x-axis of the lower part of Q_{f_1} between t_1 and t_{p_1}, the upper part of Q_{f_2} between t_{p_2} and t_2 and finally, the lower part of Q_{f_2} between t_{sep} and t_{p_2}. We also define $P_{Q'}^{up}$ and $P_{Q'}^{dw}$ as the estimated polynomials of both sides of Q' when $Q'_{lam} \leqslant Q_{min}$, where Q' is the truncated part of the hydrograph at Q_{min} level (*see* bold blue line in Fig. 2). The resolution of the polynomials' integrals A_1 and A_2 equality gives directly, thanks to the rotation, a discharge value which then has to be translated back and rotated clockwise by 90° to obtain Q'_{lam} and the corresponding time t'_{lam}.

Algorithm 1 Water volume estimation

1: Determine $t_1, t_2, t_{sep}, Q_{p_1}, Q_{p_2}, V_1, V_2, V'_1, V'_2$ and Q_{min}.
2: Perform the 90 °counterclockwise rotation and the translation.
3: Estimate $P_{f1}^{up}, P_{f1}^{dw}, P_{f2}^{up}, P_{f2}^{dw}, P_{Q'}^{up}$ and $P_{Q'}^{dw}$.
4: Test the volumes
  if $V_1 + V_2 \geqslant V_r$
    if $V_1 + V_2 = V_r$ **then** $Q'_{lam} = Q_{min}$
    else
      $A_1 = \int_{Q'_{lam}}^{Q_{p_1}} P_{f1}^{up}.dt + \int_{Q'_{lam}}^{Q_{p_1}} P_{f1}^{dw}.dt$
      $A_2 = \int_{Q'_{lam}}^{Q_{p_2}} P_{f2}^{up}.dt + \int_{Q'_{lam}}^{Q_{p_2}} P_{f2}^{dw}.dt$
      if $Q_{p_2} \geqslant Q_{p_1}$
        if $V'_2 > V_r$ **then**
          - solve $A_2 = V_r$
          - perform 90°clockwise rotation and the back translation
        end if
        if $V'_2 = V_r$ **then** $Q'_{lam} = Q_{p_1}$ **end if**
        if $V'_2 < V_r$ **then**
          - solve $A_1 + A_2 = V_r$
          - perform 90°clockwise rotation and the back translation
        end if
      else
        if $V'_1 > V_r$ **then**
          - solve $A_1 = V_r$
          - perform 90°clockwise rotation and the back translation
        end if
        if $V'_1 = V_r$ **then** $Q'_{lam} = Q_{p_2}$ **end if**
        if $V'_1 < V_r$ **then**
          - solve $A_1 + A_2 = V_r$
          - perform 90°clockwise rotation and the back translation
        end if
      end if
  else
    - solve $\int_{Q'_{lam}}^{Q_{min}} P_{Q'}^{up}.dt + \int_{Q'_{lam}}^{Q_{min}} P_{Q'}^{dw}.dt = V_r - (V_1 + V_2)$
    - perform 90°clockwise rotation and the back translation
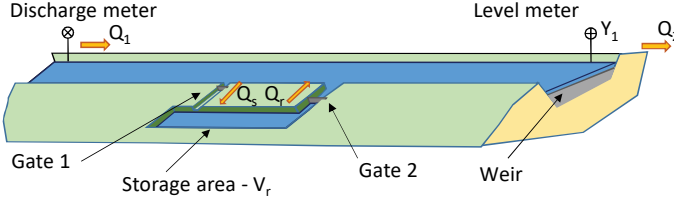 **end if**
5: return Q'_{lam} and t'_{lam}.

Fig. 3. Scheme of the studied system.

In the case of a single peak, V_1 is set equal to 0 and V_2' to V_2 in the Algorithm 1.

4. SIMULATION RESULTS

4.1 Case-study

The considered case-study is a realistic system with real hydrographs. The hydrographs are those of the Liane river located in the north of France. They are from a data base provided by the DREAL SPC (french regional environment, planning and housing agencies in charge of flood forecasting). Only a part of the Liane river is considered as a simple reach. It is equipped with a discharge meter upstream, a weir and a level meter downstream. An assumption on the presence of a flood storage area is made. The studied system is depicted in Fig. 3. The discharge meter provides the discharge Q_1; Q_2 corresponds to the weir discharge downstream. The measurement of the downstream level, Y_1, is given by the level meter. Finally, the discharge that supplies the storage area thanks to the gate 1 is denoted Q_s, and the discharge emptying it, thanks to the gate 2, is denoted Q_r.

At the end of the reach, the free flow weir aims at keeping the level of the reach Y_1 around the nominal level. Its dynamics is modelled according to the relation (2) (Litrico and Fromion, 2009)-page 160.

$$Q_2 = C_d \sqrt{2.g}(Y_1 - W_s)^{3/2} \qquad (2)$$

with W_s the sill elevation of the weir, Y_1 the water level upstream the weir, g the gravitational acceleration and C_d a coefficient that is tune to 0.6. The dynamics of the gates 1 and 2 are not modelled in this paper. It is supposed that between to simulation steps, the gates can be operated to obtain the desired discharges.

The system is modelled as a reach with a constant profile section, which characteristics are given in Table 1. The n_r [$s/m^{1/3}$] is the Manning's roughness coefficient; m (dimensionless) is the side slope of the cross section ($m = 0$ for rectangular shape), W [m] is the average width of the reach; s_b is the bottom slope. Note that the nominal discharge is Q_0.

Table 1. Physical characteristics of the reach.

n_r	m	W	Q_0	D	L
0.035	0	20	1	0.3	26.720

ID models (Schuurmans et al., 1999) are used to simulate the dynamics of the reach such as:

$$\begin{bmatrix} Y_u(s) \\ Y_1(s) \end{bmatrix} = \begin{bmatrix} p_{11}(s) & p_{12}(s) & p_{13}(s) \\ p_{21}(s) & p_{22}(s) & p_{23}(s) \end{bmatrix} \begin{bmatrix} Q_1(s) \\ Q_s^*(s) \\ Q_2(s) \end{bmatrix} \qquad (3)$$

where Y_u is the level upstream, $Q_s^*(s) = Q_s(s) + Q_r(s)$ is equal to the sum of the discharge Q_s that supplies the storage area and the discharge Q_r that empties the storage area. That implies that

these discharges are signed depending if they add or subtract discharge to the reach. In this paper, it is supposed that the gates 1 (storage) and 2 (realease) are very close and consequently no dynamic or delay has to be taken into account. The transfer functions $p_{ji}(s)$ are expressed as:

$$p_{ji}(s) = \frac{1}{A_{ji}.s}e^{-\tau_{ji}.s} \qquad (4)$$

with A_{ji} the integrator gain and τ_{ji} the delay between points j and i.

The parameters of the transfer functions p_{ji} are computed according to the characteristics of the reach. To overcome the possible overlapping in the computation of these transfer functions, a strategy that consists in using the most distant part of the reach is proposed in (Segovia et al., 2018). The coefficients of the transfer functions p_{ji} are given in Table 2, where the delays are given in seconds and A is approximated as the area of the canal, $i.e.$ $A = 20 \times 26720 = W \times L$.

Table 2. ID parameters.

	$p_{11}(s)$	$p_{12}(s)$	$p_{13}(s)$	$p_{21}(s)$	$p_{22}(s)$	$p_{23}(s)$
A_{ji}	A	A	A	A	A	A
τ_{ji}	0	5615	17069	14072	9443	0

The ID models are implemented in Matlab/Simulink to reproduce the dynamics of the studied system. The real hydrographs Q_1 are the inputs of the simulated model. Finally, Y_1 downstream is the reference level for the flood impact. The flood mitigation control strategy consists in opening or closing the gates 1 and 2 according to the defined Logic Control rules by considering the type and magnitude of the hydrograph and the capacity of the storage area.

For this system, the capacity of the flood storage area corresponds to $1,000,000$ m^3. It is a fictive flood storage area. The nominal level of the reach corresponds to 0.3 m. It is supposed that a flood occurs when this level exceeds 0.6 m. A level higher than 0.8 m leads to a strong flood. These alarm levels are also fictive and were selected according to the identified model of the reach. Finally, the threshold Q_{lam} is tuned according to a 2-year flood, $i.e.$ $Q_{lam} = 10$ m^3/s.

4.2 Scenarios of flood

Three scenarios based on three real hydrographs are considered. The first one, $scenario$ 1 is a single peak with a highest discharge Q_1 upper than 43 m^3/s (see Fig. 4.b). In the following figures, the simulation results are depicted in solid blue line when no storage area is considered, in dotted magenta line when $Q_{lam} = 10$ m^3/s is considered, and in dashed red line for the optimal Q_{lam}' that is determined by the designed flood mitigation control strategy. In the scenario, it leads to $Q_{lam}' = 15.13$ m^3/s. In the first case, when no storage area is available, the level downstream Y_1 reaches more than 0.8 m causing extreme flood (see blue line in Fig. 4.a). Y_1 is limited to 0.66 m when the storage area is used with $Q_{lam} = 10$ m^3/s (see dotted magenta line in Fig. 4.a) causing flood. In this case, the storage area is supplied too early as it is depicted in Fig. 4.c, $i.e.$ from the 31th hour. That leads to fill the storage area from the 46th hour (see dotted magenta line in Fig. 4.e) and finally this induces another discharge peak downstream on Q_2 from the 52 hour (see dotted magenta line in Fig. 4.d). By using Q_{lam}', the storage area is supplied later, from the 34th hour (see dashed red line in Fig. 4.c) leading to a maximal $Y_1 = 0.49$ m, thus avoiding the flood.
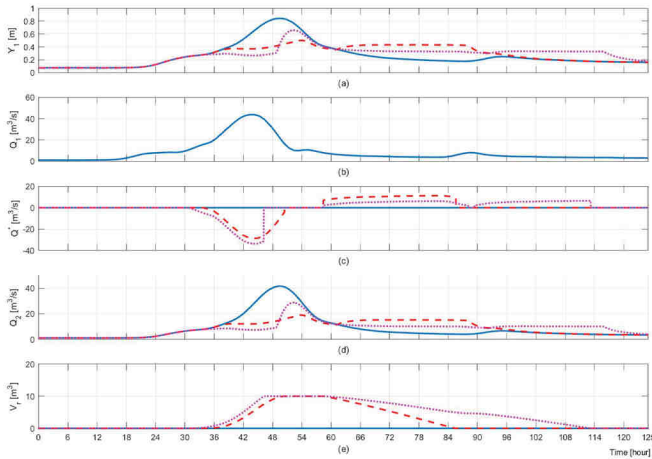
Fig. 4. *Scenario* 1 with a) Y_1 the level downstream, b) Q_1 the real hydrograph upstream, c) Q^* the discharge in and from the storage area, d) Q_2 the discharge downstream and e) V_r the volume in the storage area.
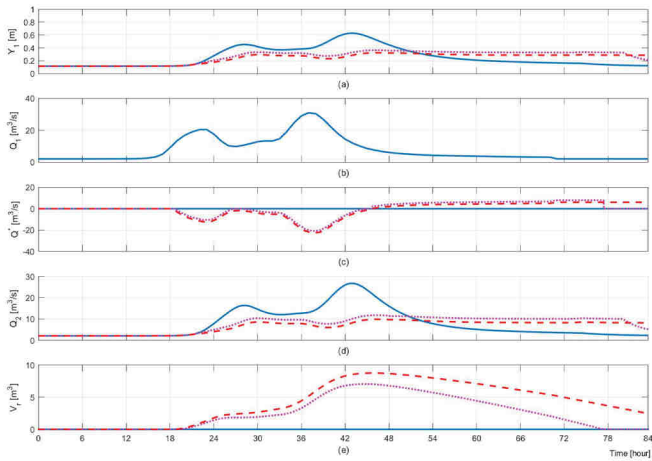

Fig. 5. *Scenario* 2 with a) Y_1 the level downstream, b) Q_1 the real hydrograph upstream, c) Q^* the discharge in and from the storage area, d) Q_2 the discharge downstream and e) V_r the volume in the storage area.

By the following, when the discharge Q_1 is lower than 8 m^3/s, the storage area is emptying started from the 52 hour (*see* Fig. 4.c).

The two others scenarios correspond to hydrographs with a double peak. In *scenario* 2 the magnitude of the first peak is lower than the second one (*see* Fig. 5.b), with a maximal value of Q_1 upper than 31 m^3/s. When no storage area is available, the level downstream Y_1 exceeds 0.6 m causing flood (*see* blue line in Fig. 5.a). In this scenario, the volume from the hydrograph is less than the total volume of the storage area. Therefore, all the water volume can be routed to the storage area avoiding flood even for $Q_{lam} = 10$ m^3/s (*see* dotted magenta line in Fig. 5.a), without completely filling the storage area (*see* dotted magenta line in Fig. 5.e). The designed flood mitigation control strategy leads to a value $Q'_{lam} = 8,25$ m^3/s that allows optimizing the use of the storage area; as it can be observed by comparing the curves in dotted magenta and dashed red lines in Fig. 5.e. By using Q'_{lam}, the gain on the maximum value of Y_1 is equal to 0.04 m, and on Q_2 to 1.7 m^3/s (*see* Fig. 5.d).
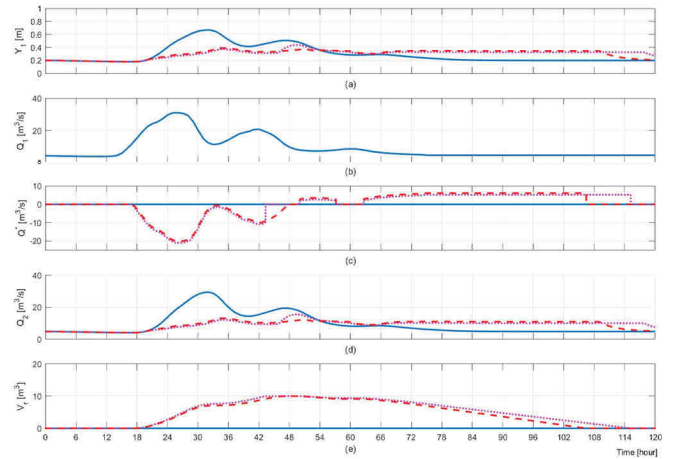

Fig. 6. *Scenario* 3 with a) Y_1 the level downstream, b) Q_1 the real hydrograph upstream, c) Q^* the discharge in and from the storage area, d) Q_2 the discharge downstream and e) V_r the volume in the storage area.

In *scenario* 3 the magnitude of the first peak is higher than the second one (*see* Fig. 6.b), with a maximal value of Q_1 upper than 31 m^3/s. Here again, when no storage area is available, the level downstream Y_1 exceeds 0.6 m causing flood (*see* blue line in Fig. 6.a). However, even if the maximal value of Q_1 is very similar for both scenarios, *scenario* 2 and *scenario* 3, the duration of the peaks in *scenario* 3 is much longer than in *scenario* 2. That means that the storage area is totally full for $Q_{lam} = 10$ m^3/s at time 43 hour (*see* dotted magenta line in Fig. 6.e) and it is no more possible to use the storage area. Consequently, the level Y_1 exceeds 0.48 m at time 49 hour (*see* dotted magenta line in Fig. 6.a). The designed flood mitigation control strategy leads to a value $Q'_{lam} = 10.9$ m^3/s that allows starting supplying the storage area, little time later (*see* dashed red line in Fig. 6.c). Thanks to this delay, the level Y_1 is keeping lower than 0.4 m. The discharge Q_2 is also keeping lower than 13 m^3/s (*see* Fig. 6.d).

The results of these three scenarios highlight the benefits of using an optimal flood mitigation control strategy. Even for the scenarios with double peaks and a discharge magnitude around 30 m^3/s, the gain can be observed. This gain is much more important for hydrographs with bigger discharge magnitudes.

5. CONCLUSION

In this paper a flood mitigation control strategy is designed. It requires the availability of flood storage areas, discharge and level meters. The designed strategy is based on the prediction of hydrographs, the estimation of the water volume, and the determination of the optimal time to begin the storage area supplying. An algorithm that leads to the determination of the water volume according to hydrographs is described. A realistic case-study based on real hydrographs is used to simulate three scenarios and to show the advantages of the designed flood mitigation control strategy. Future works will consider the uncertainties in the forecasting of rainfall/runoff models and therefore on the hydrographs.

REFERENCES

Asefa, T., Kemblowski, M., McKee, M., and Khalil, A. (2006). Multi-time scale stream flow predictions: The support vector machines approach. *Journal of Hydrology*, 318(1), 7 – 16.

Bastin, G., Moens, L., and Dierick, P. (2009). Online river flow forecasting with hydromax : successes and challenges after twelve years of experience. *In proceedings of the 15th IFAC Symposium on System Identification, Saint-Malo, France, July 6-8.*

Bencheikh, G., Tahiri, A., Chiron, P., Archimède, B., and Martignac, F. (2017). A flood decrease strategy based on flow network coupled with a hydraulic simulation software 11this work was partially supported by the urban community of le grand tarbes. *IFAC-PapersOnLine*, 50(1), 3171 – 3176. doi:https://doi.org/10.1016/j.ifacol.2017.08.337. 20th IFAC World Congress.

Breckpot, M., Agudelo, O.M., and Moor, B.D. (2013). Flood control with model predictive control for river systems with water reservoirs. *Journal of Irrigation and Drainage Engineering*, 139(7), 532–541. doi:10.1061/(ASCE)IR.1943-4774.0000577.

Chang, F.J. and Chang, Y.T. (2006). Adaptive neuro-fuzzy inference system for prediction of water level in reservoir. *Advances in Water Resources*, 29(1), 1 – 10.

Che, D. and Mays, L.W. (2017). Application of an optimization/simulation model for real-time flood-control operation of river-reservoirs systems. *Water Resources Management*, 31(7), 2285–2297. doi:10.1007/s11269-017-1644-3.

Delgoda, D.K., Saleem, S.K., Halgamuge, M.N., and Malano, H. (2013). Multiple model predictive flood control in regulated river systems with uncertain inflows. *Water Resources Management*, 27(3), 765–790. doi:10.1007/s11269-012-0214-y.

Duviella, E. and Bako, L. (2012). Predictive black-box modeling approaches for flow forecasting of the liane river. *SYSID12, Bruxelles, Belgium,.*

Duviella, E., Doniec, A., and Nouasse, H. (2018). Adaptive water-resource allocation planning of inland waterways in the context of global change. *Journal of Water Resources Planning and Management*, 144(9), 04018059. doi:10.1061/(ASCE)WR.1943-5452.0000970.

Elshorbagy, A., Corzo, G., Srinivasulu, S., and Solomatine, D.P. (2010). Experimental investigation of the predictive capabilities of data driven modeling techniques in hydrology - part 2: Application. *Hydrology and Earth System Sciences*, 14(10), 1943 – 1961.

Feng, L.H. and Lu, J. (2010). The practical research on flood forecasting based on artificial neural networks. *Expert systems with Applications*, 37, 2974 – 2977.

Hadid, B., Duviella, E., and Lecoeuche, S. (2018). Improvement of a predictive data-driven model for rainfall-runoff global characterization of aa river. *Proceedings of the 4th International Forum on Research and Technologies for Society and Industry, Palermo, Italy.*

IPCC (2018). *Global warming of 1.5C*. The Intergovernmental Panel on Climate Change.

Labadie, J.W. (2004). Optimal operation of multireservoir systems: State-of-the-art review. *Journal of Water Resources Planning and Management*, 130(2), 93–111. doi:10.1061/(ASCE)0733-9496(2004)130:2(93).

Litrico, X. and Fromion, V. (2009). *Modeling and Control of Hydrosystems*. Springer London. doi:10.1007/978-1-84882-624-3.

Mustafa, A., Bruwier, M., Archambeau, P., Erpicum, S., Pirotton, M., Dewals, B., and Teller, J. (2018). Effects of spatial planning on future flood risks in urban environments. *Journal of Environmental Management*, 225, 193 – 204. doi:

https://doi.org/10.1016/j.jenvman.2018.07.090.

Nouasse, H., Chiron, P., and Archimède, B. (2013). Transportation network model with time delay for flood lamination strategy. In *2013 XXIV International Conference on Information, Communication and Automation Technologies (ICAT)*, 1–7. doi:10.1109/ICAT.2013.6684091.

Perrin, C. and Andréassian, V. (2001). Does a large number of parameters enhance model performance ? comparative assessment of common catchment model structures on 429 catchments. *Journal of Hydrology*, 242(3-4), 275–301.

Perrin, C., Michel, C., and Andréassian, V. (2003). Improvement of a parsimonious model for streamflow simulation. *Journal of Hydrology*, 279, 275 – 289.

Previdi, F. and Lovera, M. (2009). Identification of parametrically-varying models for the rainfall-runoff relationship in urban drainage networks. *IFAC Proceedings Volumes*, 42(10), 1768 – 1773. 15th IFAC Symposium on System Identification.

Raso, L., Chiavico, M., and Dorchies, D. (2019). Optimal and centralized reservoir management for drought and flood protection on the upper seine-aube river system using stochastic dual dynamic programming. *Journal of Water Resources Planning and Management*, 145(3), 05019002. doi:10.1061/(ASCE)WR.1943-5452.0001040.

Romanowicz, R., Young, P., Beven, K., and Pappenberger, F. (2008). A data based mechanistic approach to non-linear flood routing and adaptive flood level forecasting. *Advances in Water Resources*, 31(8), 1048 – 1056.

Sauquet, E. and Lang, M. (2017). 18 - flood regimes: Recent development and future under climate change. In F. Vinet (ed.), *Floods*, 299 – 309. Elsevier. doi:https://doi.org/10.1016/B978-1-78548-268-7.50018-3.

Schuurmans, J., Clemmens, A.J., Dijkstra, S., Hof, A., and Brouwer, R. (1999). Modeling of irrigation and drainage canals for controller design. *Journal of irrigation and drainage engineering*, 125(6), 338–344.

Segovia, P., Rajaoarisoa, L., Nejjari, F., Puig, V., and Duviella, E. (2018). Modeling of interconnected flat open-channel flow: Application to inland navigation canals. In P. Gourbesville, J. Cunge, and G. Caignaert (eds.), *Advances in Hydroinformatics*, 75–90. Springer Singapore, Singapore.

Shenava, N. and Shourian, M. (2018). Optimal reservoir operation with water supply enhancement and flood mitigation objectives using an optimization-simulation approach. *Water Resources Management*, 32(13), 4393–4407. doi:10.1007/s11269-018-2068-4.

Vermuyten, E., Meert, P., Wolfs, V., and Willems, P. (2018). Model uncertainty reduction for real-time flood control by means of a flexible data assimilation approach and reduced conceptual models. *Journal of Hydrology*, 564, 490 – 500. doi:https://doi.org/10.1016/j.jhydrol.2018.07.033.

Wolfs, V., Meert, P., and Willems, P. (2015). Modular conceptual modelling approach and software for river hydraulic simulations. *Environmental Modelling & Software*, 71, 60 – 77.

Young, P. (2003). Top-down and data-based mechanistic modelling of rainfall-flow dynamics at the catchment scale. *Hydrological Processes*, 17, 2195 – 2217.

Zhang, X., Luo, J., Sun, X., and Xie, J. (2019). Optimal reservoir flood operation using a decomposition-based multi-objective evolutionary algorithm. *Engineering Optimization*, 51(1), 42–62. doi:10.1080/0305215X.2018.1439942.